Geologie en Mijnbouw **70**: 145–161, 1991.

Geometries of extensional fault systems, observed and mapped on aerial and satellite photographs of Central Afar (Ethiopia/Djibouti)

Peter Kronberg
Institut für Geologie, Technische Universität Clausthal, Leibnizstr. 10, D 3392 Clausthal-Zellerfeld, Germany

Received 06 June 1990; accepted in revised form 15 November 1990

Key words: Afar, crustal extension, fault tectonics, remote sensing, rift development, triple junction

Abstract

Well exposed Central Afar (Ethiopia/Djibouti) offers direct observation of a wide range of extensional structures and rift morphologies, at regional and local scale. Large Format Camera satellite photography and aerial photography was used to investigate in stereo-models phenomena of progressive extensional faulting. Representative successive fault geometries and fault evolution patterns are presented and discussed.

Introduction

In most modern and ancient rifts extensional fault geometries and fault evolution patterns related to early and successive stages of rift development are obscured by advanced crustal deformation and rift sedimentation. Hence, during the last decade, sandbox- and computer modelling was used to increase our understanding of extensional processes and models of rift development were derived from geophysical and borehole data from various (mostly advanced) continental rift systems. (Wernicke & Burchfiel 1982, Jackson & McKenzie 1983, Bosworth 1985, Rosendahl 1987, McClay & Ellis 1987, Morley 1988, Cochran & Martinez 1988, Ebinger 1989).

Central Afar (Ethiopia/Djibouti, see Fig. 1a) offers direct observation of a wide range of extensional structures and rift morphologies representing different stages of upper crustal deformation, at regional and local scale. In fact, as part of an advanced and still active continental rift system and triple junction of three major rift zones (Red Sea-, Aden- and Ethiopian Rifts, see Fig. 1b) well exposed arid Central Afar can be regarded as a natural (realistic) model of upper crustal deformation under progressive and still active rifting. Therefore, it seemed a suitable place to investigate phenomena of successive extensional faulting at local and regional scale, along- and across-strike.

Complete coverage of Central Afar by satellite and aerial photography allowed observation and mapping of extensional structures in stereo models (under a mirror stereoscope). In a first step, synoptical Large Format Camera (LFC) photography (approx. scale 1:800 000, spatial resolution about 15 m) was used to map extensional structures of Central Afar (map area shown in Fig. 1a, Fig. 11 and 12). Then, aerial photography (approx. scale 1:50 000, spatial resolution about 5 m) was used to map and evaluate extensional fault geometries and fault patterns of selected areas characterized by different styles and stages of extensional deformation. Finally, relations and interactions between local and regional extensional fault systems were studied in satellite and aerial photography. A set of aerial photographs, map views and structural cross sections was compiled to illustrate observed geometries of extensional fault systems and successive stages of extensional upper crustal deformation.

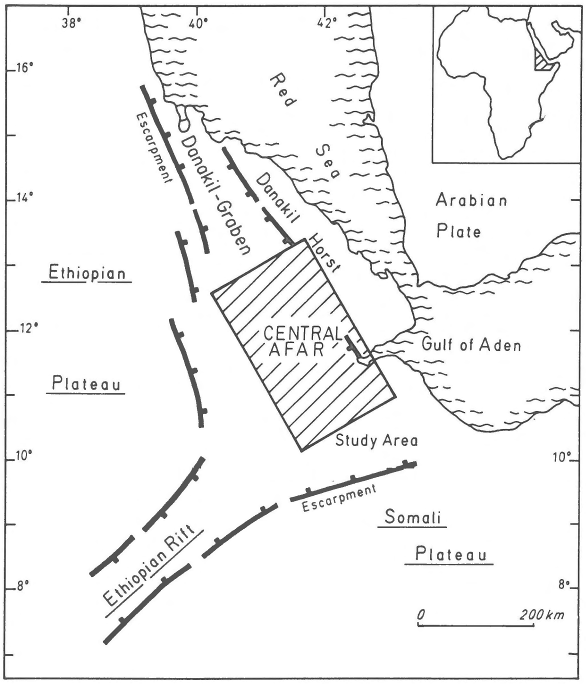

Fig. 1a. Locality map of study area.

Unfortunately, for technical reasons, not all presented examples of aerial and satellite photography can be shown at original scale or as stereo-models.

Early stages of extensional faulting

Aerial photography from NW-SE striking active Manda Haro- and Assal-Ghoubbet Rifts (situated at the northwestern and south-eastern margins of Central Afar, respectively; see Fig. 1b: M.H. and Assal-Gh.R.) indicates that upper crustal extension initiates as isolated fractures, mostly curvilinear and in a diffuse en échelon arrangement subparallel to the rift axis. This is demonstrated in an oblique aerial photograph from Assal-Ghoubbet Rift (Fig. 2a) showing NW-striking surface ruptures formed in 1978 in young rift basalts and in vertical aerial photography from the axial zone of Manda Haro Rift (Fig. 2b). Here, subrecent curvilinear fissures in diffuse en échelon arrangement outline incipient boundary faults of a future graben. The axis of crustal subsidence is marked by the direction of a subrecent lava flow and by the location of a lake. Ongoing extension would lead to the lateral propagation and coalescence of shown early fractures, to further subsidence of the graben floor and to development of master and subsidiary faults as displayed in map view of a well developed symmetric graben (Fig. 2c; part of the southern Danakil-Graben system). The spatial occurrence of its faults as well as fault geometry and the shape of fault-bounded larger and smaller crustal blocks (wedge- or rhomboid shaped) do correspond quite well to early patterns of extensional fracturing as illustrated in Fig. 2a and Fig. 2b. According to comparative studies of extensional fault geometries of Central Afar Fig. 2 illustrates in 3 successive steps basic geometries of extensional fault systems that do occur at local and regional scale. (compare fault geometries and shape of fault bounded crustal blocks in Fig. 3a–c, Fig. 5a and Fig. 9).

Aerial views of an area NW of Sardo (Fig. 3a–c) illustrate successive steps in the development of a complex sinuous fault pattern and its associated horst/graben structures. In the area of Fig. 3a diffuse crustal extension has led to formation of planar and curviplanar steep normal faults of finite length. Shadowed or illuminated fault scarps indicate opposing directions of dip and throw and lateral differences in throw. The early extensional fracture pattern of Fig. 3a, already, displays some characteristic phenomena of later sinuous fault patterns, such as overlapping and interfingering of planar and curviplanar faults with equal, opposing or alternating directions of dip and throw, along- and across strike. In Fig. 3b further extension has led to lateral propagation of pre-existing faults, the link-up of formerly isolated curviplanar faults and the formation of major (more extensive) faults with larger throw (often, in en échelon arrangement; see upper part of Fig. 3b). Locally, incipient sedimentary basins have developed on subsiding or downwarped fault blocks. In Fig. 3c (situated adjacent to the area of Fig. 3b along strike, towards lower left) even stronger crustal extension has been compensated by strong movements of individual faults blocks or series of larger and smaller fault blocks across steep curviplanar normal fault of finite length. Differential subsidence of typical wedge- or rhomboid shaped fault blocks, along and

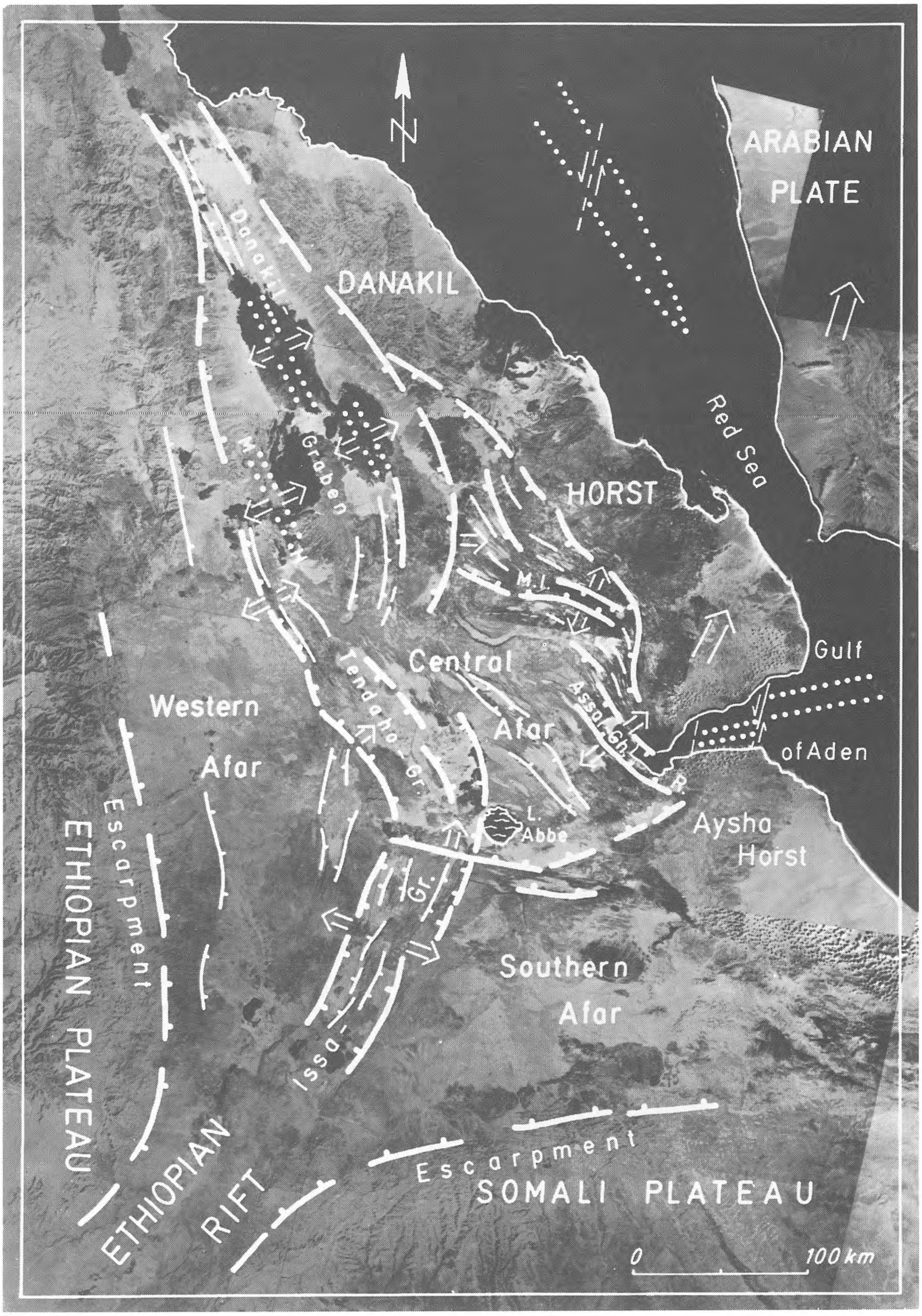

Fig. 1b. Structural setting and major geological units of the Afar and adjacent areas (superimposed on a Landsat MSS mosaic). M.I.: Manda Inakir spreading zone; Assal – Gh. R.: Assal Ghoubet Rift; M.H.: Manda Haro spreading zone. (The three active spreading zones of Central Afar).

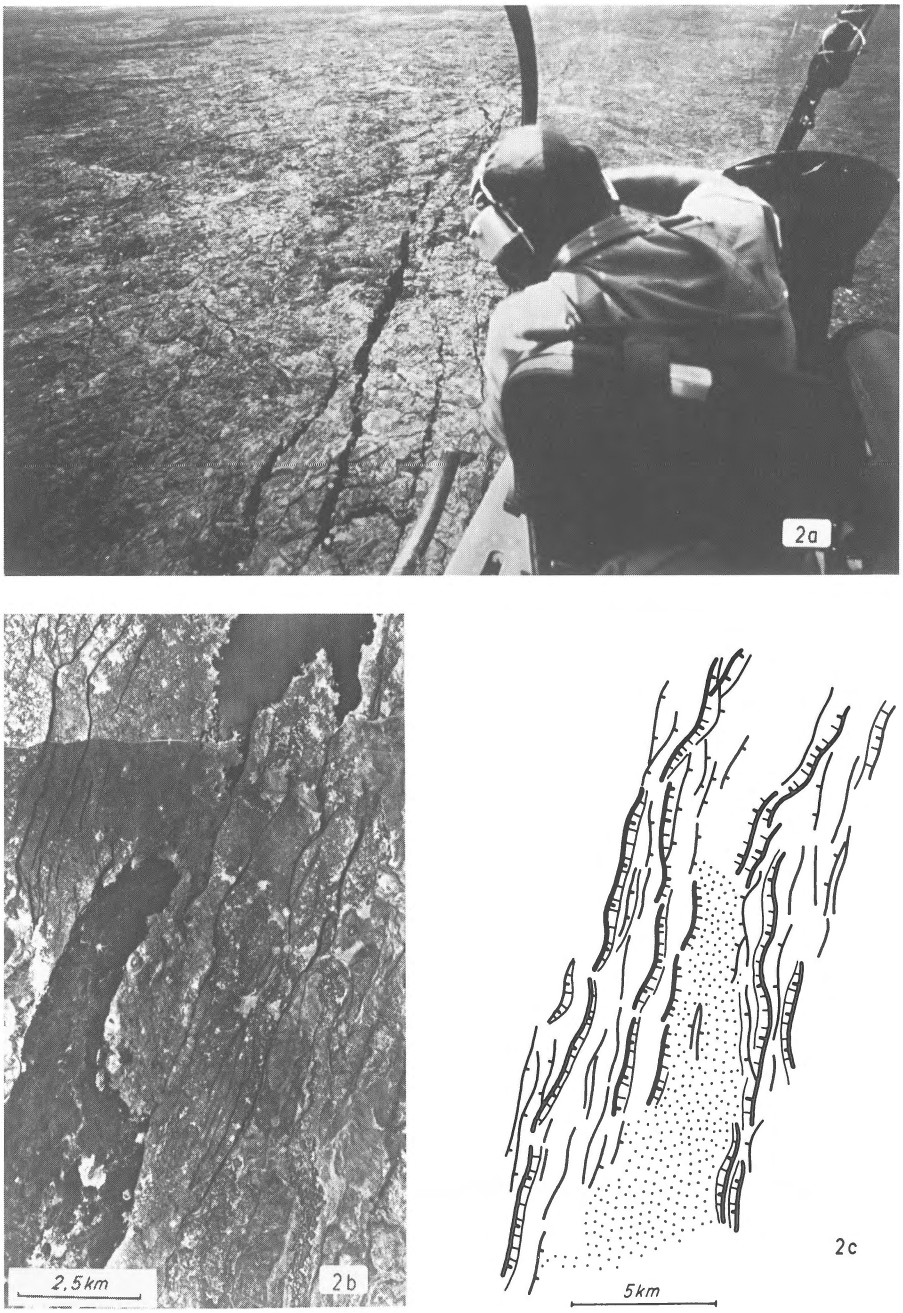

Fig. 2. Early extensional fracturing and later fault development patterns. Isolated curvilinear and linear fractures, fissures and faults characterize an initial stage of upper crustal break up as shown in an oblique photo at the NNW striking axial zone of Assal-Ghoubet Rift (Fig. 2a; photo from George 1982). In a vertical aerial photograph from Manda Haro spreading zone Fig. 2b displays an early sinuous fault pattern outlining border faults of an incipient graben structure subparallel to the rift axis. For comparison Fig. 2c: map view of a major graben structure (Southern Danakil Graben). Note the geometric similarities of early extensional fracture pattern and later extensional structures.

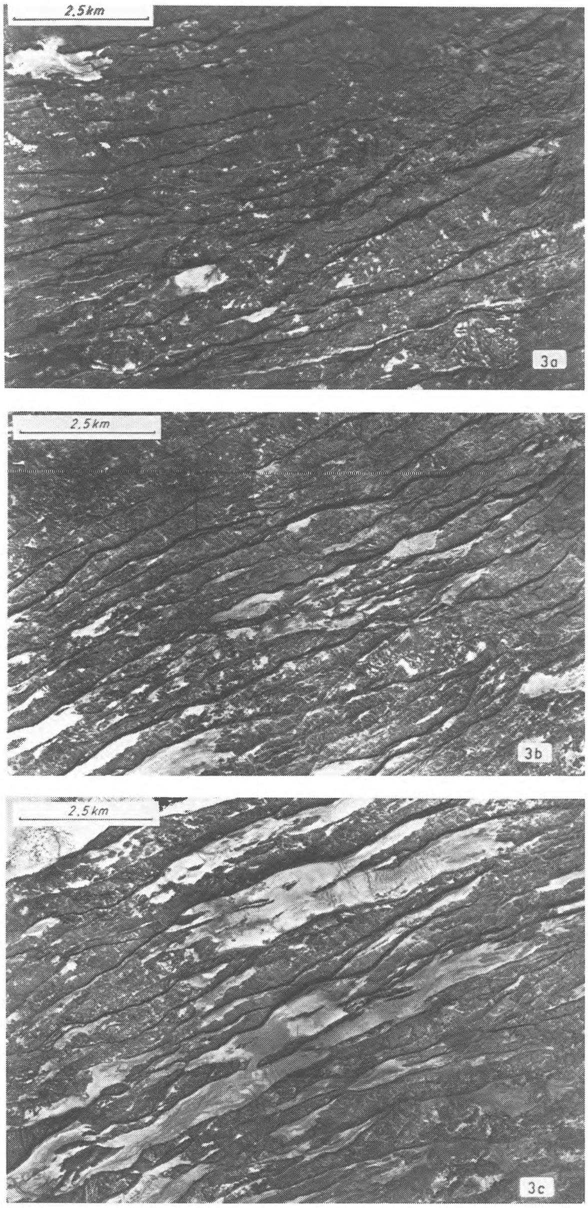

Fig. 3. Three successive stages in the development of a complex sinuous fault pattern and associated horst/graben structures (occuring, along strike, about 25 km NW of Sardo). Fault scarps in shadow or illuminated according to direction of dip and throw.

across strike, resulted in the development of larger and smaller horst and graben structures and of sedimentary basins.

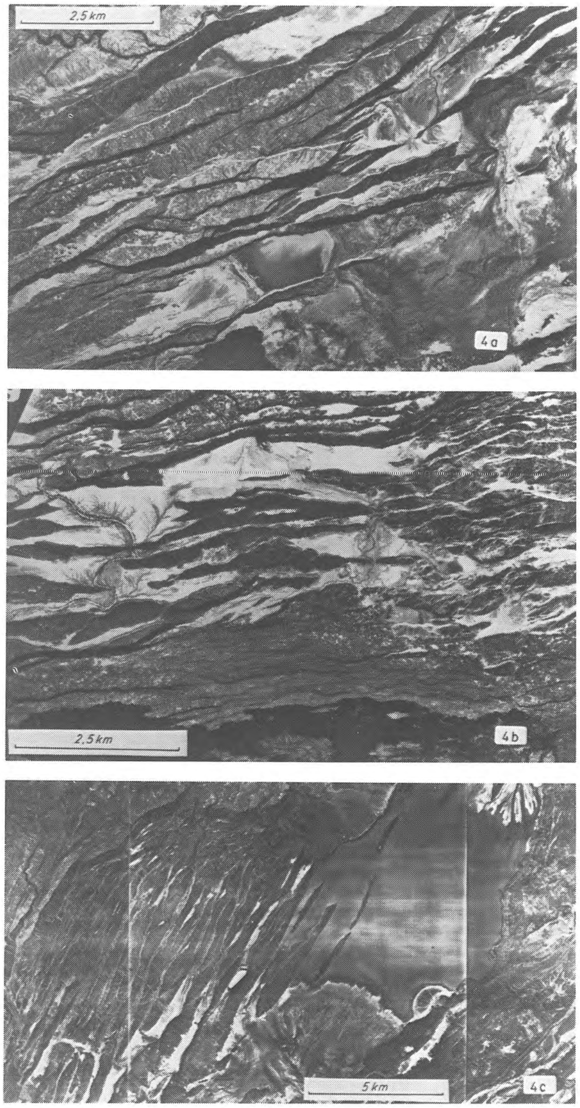

Fig. 4. Three examples of more advanced stages of extensional deformation.

a: Rotation, bending, twisting and plunging of fault blocks within a preexisting fault pattern reveal progressive extensional deformation leading to domino-type structures (in the upper right corner). Fault scarps in shadow or illuminated according to direction of dip and throw.

b: A zone of uptilted extensional fault blocks (domino- or book-shelve type) indicating rotational faulting.

c: En-échelon set high angle normal faults (upper left) bordering an extensional unit characterized by progressive rotation of fault blocks across a suspected listric detachment fault (at lower right). All examples are from active Manda-Haro spreading zone.

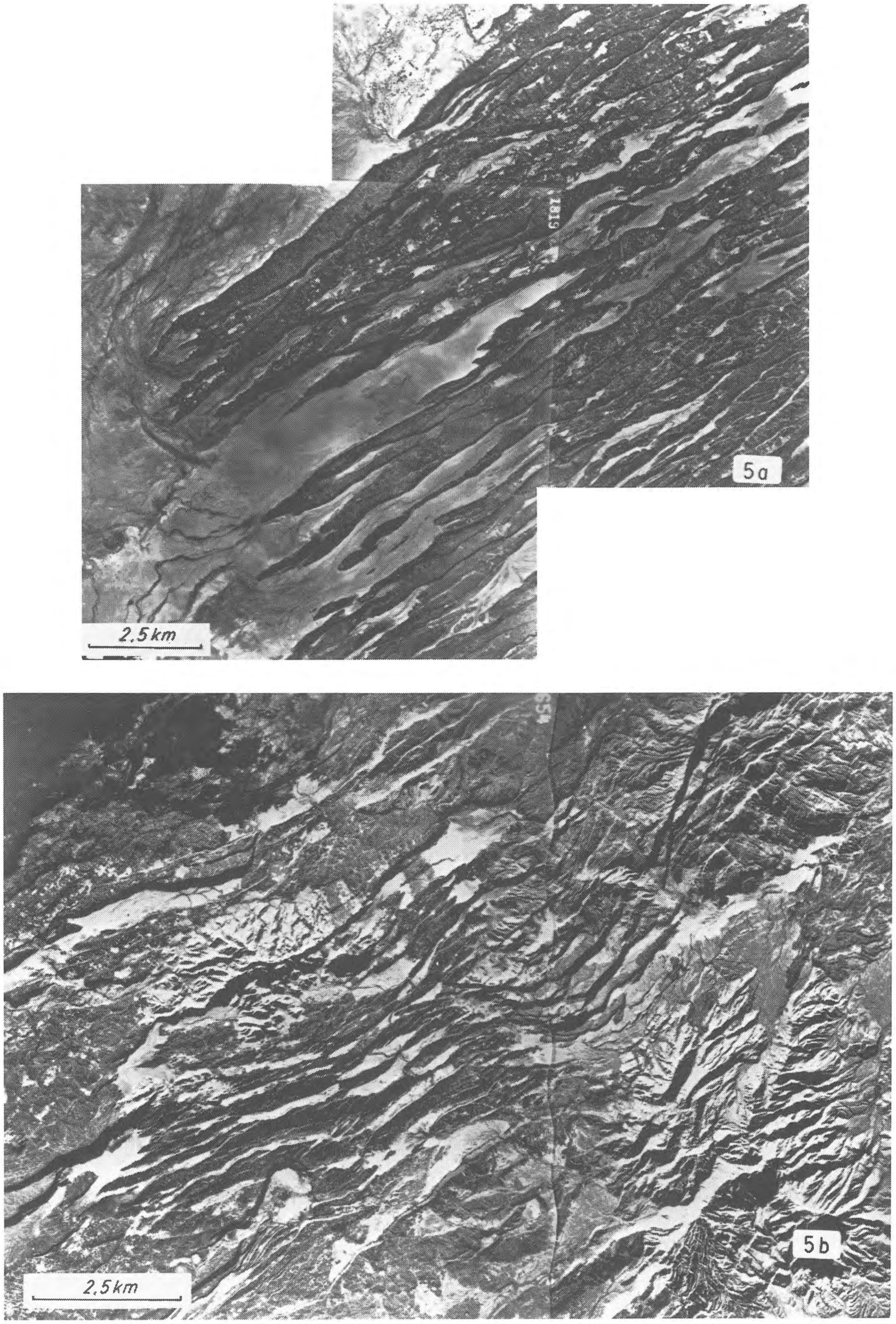

Fig. 5. Two examples of advanced extensional deformation.
a: Widespread (diffuse) extensional faulting led to horst/graben rift topography. Later crustal subsidence caused plunging of fault block units towards lower left.
b: A well defined zone characterized by rotation of imbricate fault blocks (with alternating direction of dip and throw along strike) indicates concentration of extensional stress into a narrow crustal zone bordered by high angle normal faults in en échelon arrangement (Fault scarps in shadow or illuminated according to direction of dip and throw).

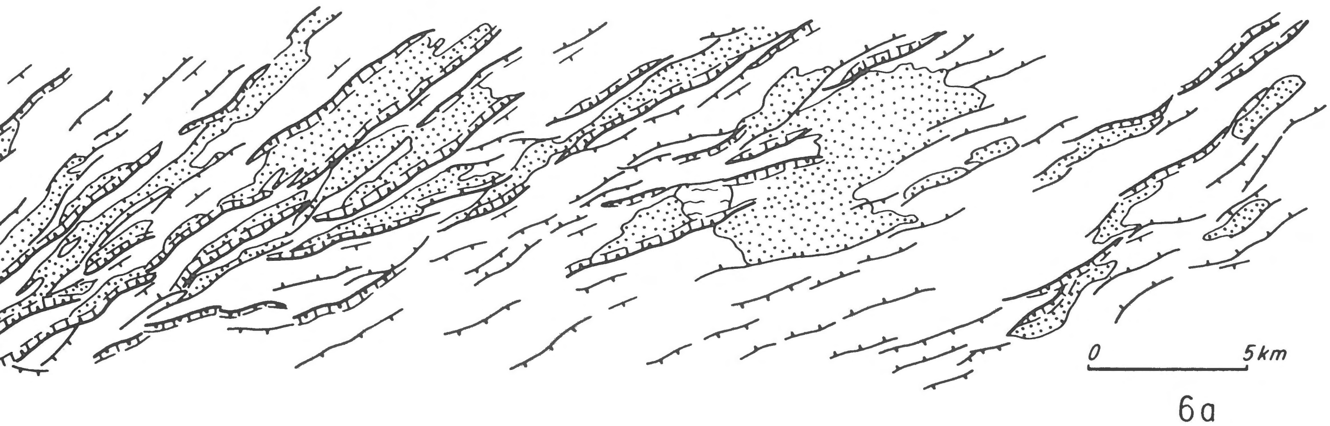

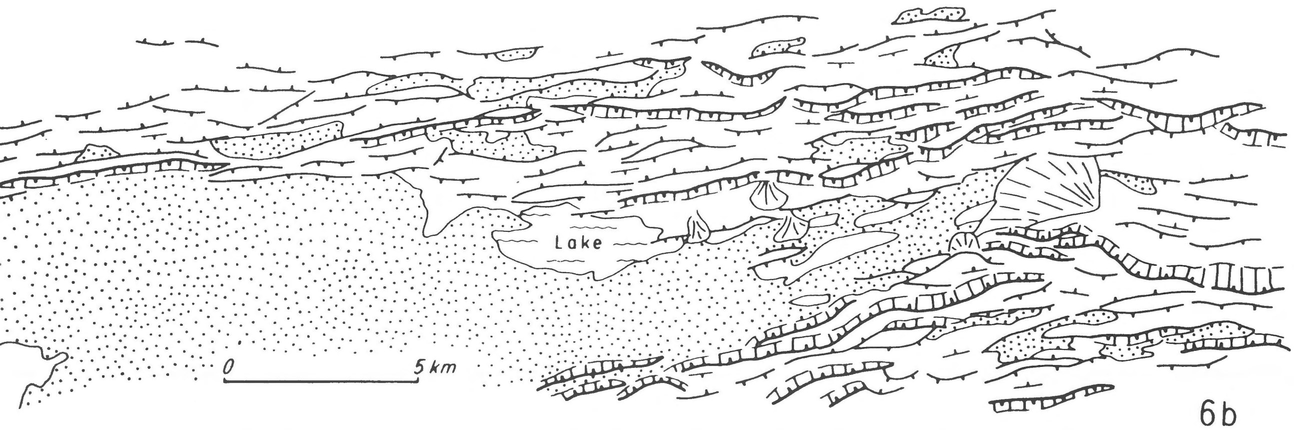

Fig. 6. a: Map view of an area of widespread extensional faulting with typical horst/graben structures (NW of Sardo).
b: Part of a major graben structure with high angle normal master faults and associated synthetic and antithetic subsidiary fault pattern (Southern Danakil Graben).

More advanced stages of upper crustal extensional deformation

Comparative studies of extensional structures in stereo-models from Central Afar show, clearly, that ongoing higher extensional stress leads to progressive motion and deformation of pre-existing (wedge- or rhomboid shaped) fault blocks or series of fault blocks across steep normal faults (compare Morton & Black 1975). Lateral changes of extensional stress will result in different styles and stages of upper crustal deformation, along and across strike, within a given rift system.

Fig. 4a shows an area where differential subsidence along and across strike and lateral changes in throw have caused bending, plunging and twisting of individual fault blocks or fault block sequences. The major part of Fig. 4a is still characterized by non- rotational faulting (rotation of fault blocks but no rotation of pre-existing faults under continuous extension). Just in the upper right part of Fig. 4a there is a sequence of uniformly uptilted fault blocks (block surfaces in shadow, fault scarps illuminated), indicating rotational faulting (with rotation of pre-existing faults) and high extensional strain. Fig. 4a demonstrates that different extensional mechanisms can operate within a given extensional system along strike due to lateral differences in extensional stress.

Across-strike differences in extensional deformation are shown in Fig. 4b. Along its central part one can observe a 2,5 km wide zone of uptilted

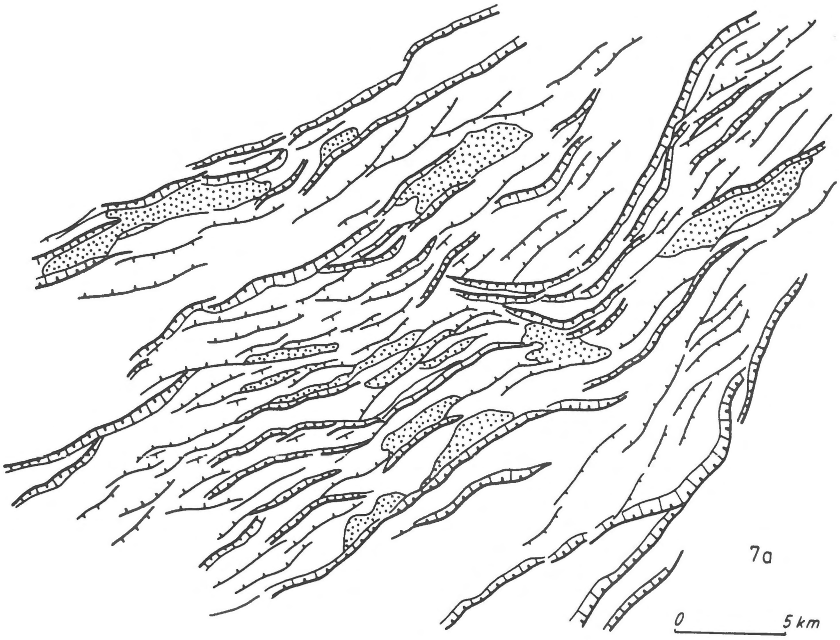

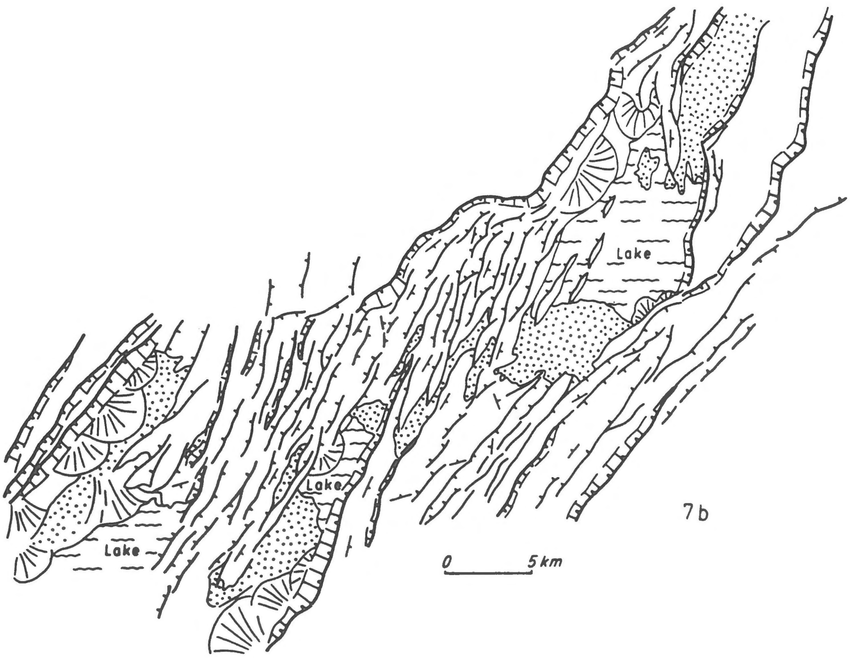

Fig. 7. Map views of along strike complications in areas of advanced extensional faulting.
a: display of neighboured extensional units (uptilted fault block series) with different (alternating) directions of dip and throw, along strike (compare Fig. 5b).
b: En échelon setting of two major graben systems linked by a transfer zone of advanced extensional faulting compensating differential subsidence of the two grabens (Dobi- and Hanle Graben, compare Fig. 8). Note opposing direction of dip and throw of neighboured master faults, along strike (central part).

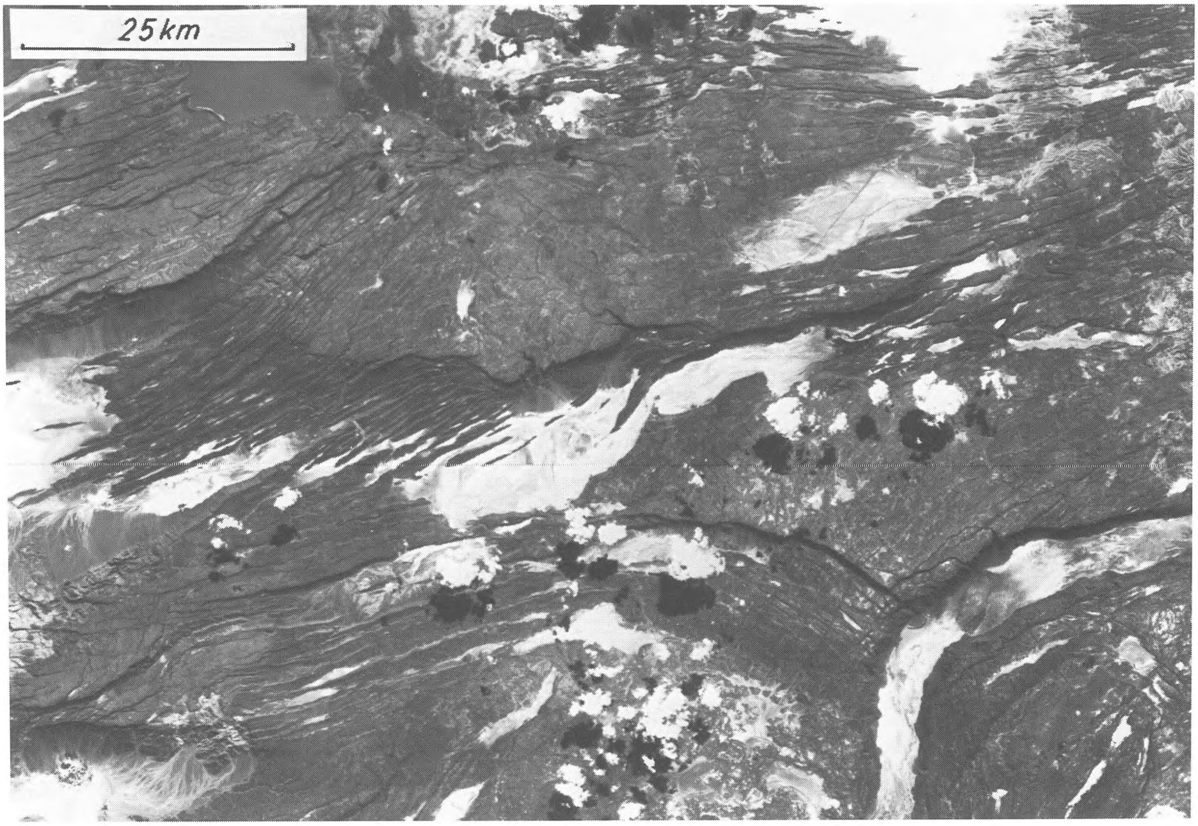

Fig. 8. Large scale extensional structures and crustal warping (characterizing an advanced rift system) shown in LFC photography from Dobi Graben and adjacent areas (further comments see text).

(rotated) fault blocks (with rotation of pre-existing curviplanar normal faults) bordered by curviplanar high angle master faults towards adjacent zones displaying lower extensional strain. On traversing such a zone of 'domino' (or 'bookshelve-') structures (centre Fig. 4b) one could expect to find the same lithostratigraphic unit in each successive fault block. The shape of the rotated fault blocks still reflects the basic geometry of a pre-existing sinuous fault pattern. Fig. 4c gives an extreme example of rotated imbricate fault blocks and of the abrupt lateral termination of domino- or bookshelve type deformation by a set of high angle normal faults.

At a large scale, tilted fault block areas or domino type domains have been observed within Central Afar along a few well defined zones (20 to 50 km in length and 6 to 12 km wide) of the Manda Haro (M.H.) Rift, the southern Danakil Graben and the Manda Inakir (M.I.) spreading zone (compare Fig. 1b). One could get the impression that high extensional stress was concentrated into relatively narrow but extensive zones during certain phases of rifting in Central Afar. Such zones are now in sharp contrast in style and stage of extensional deformation to adjacent areas characterized by relatively moderate deformation.

At a local to regional scale, Fig. 5 shows two areas of different mechanisms of extensional deformation Fig. 5a shows diffuse extensional faulting and associated horst and graben topography (compare Fig. 3). Fig. 5b is crossed, diagonally, by a well defined high strain zone characterized by rotational faulting. Of special interest here are repeated, along-strike changes in the direction of dip and throw of rotated imbricate fault block series within the high strain zone (fault scarps either illuminated or in shadow according to direction of dip and throw). En échelon set curviplanar high angle mas-

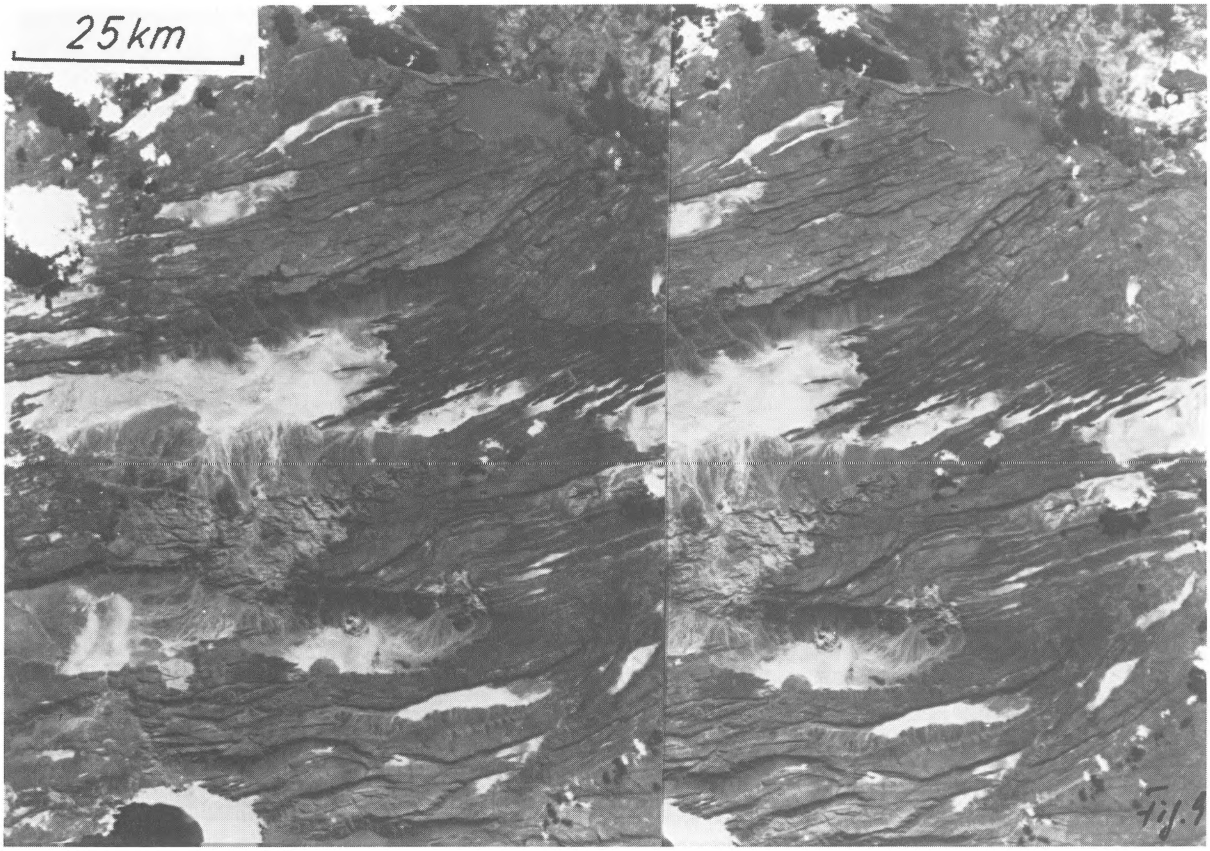

Fig. 9. Stereogram (LFC photography) illustrating advanced extensional faulting, rift topography and crustal warping of the area between Tendaho Graben (upper right) and Assal-Ghoubet Rift (lower left). Compare Fig. 11.

ter faults outline individual sections of different dip and throw.

Figs. 6 and 7 give representative map views of some typical fault patterns from Central Afar. While Fig. 6a relates to diffuse extensional faulting, Fig. 6b covers part of a major graben structure, displaying its master and subsidiary faults and fault block geometries. In both figures sedimentary basins indicate structural lows. Fig. 7a provides a map view of the high strain zone of Fig. 5b and its border faults (note change of dip and throw direction along- and across-strike). Under ongoing extension the along-strike asymmetries shown could, eventually, develop into isolated depositional systems and larger alternating half graben structures (linked by transfer or accomodation zones of complex structural setting) as described from the Tanganyika-Rift by Rosendahl (1987) and Moorley (1988) and from the Gregory Rift by Bosworth et al. (1986). Fig. 7b shows the structural setting of an area where two major en-échelon graben systems are linked by an extensional high strain zone that is characterized by intense rotational faulting. This area is shown in aerial view in Figs. 4c, 8 and 9. It could be interpreted as a transfer zone striking obliquely to the rift axis. No indication of strike slip motions has been found.

In its central part Fig. 8 shows the Dobi Graben and (towards the left) the rotated imbricate fault block sequence of the above mentioned transfer zone between Dobi- and Hanle Graben (left centre). In general, Fig. 8 provides a synoptical view of the complex extensional fault pattern that characterizes an advanced rift system: symmetric and asymmetric graben structures of different size, extensive high angle normal faults in en échelon set-

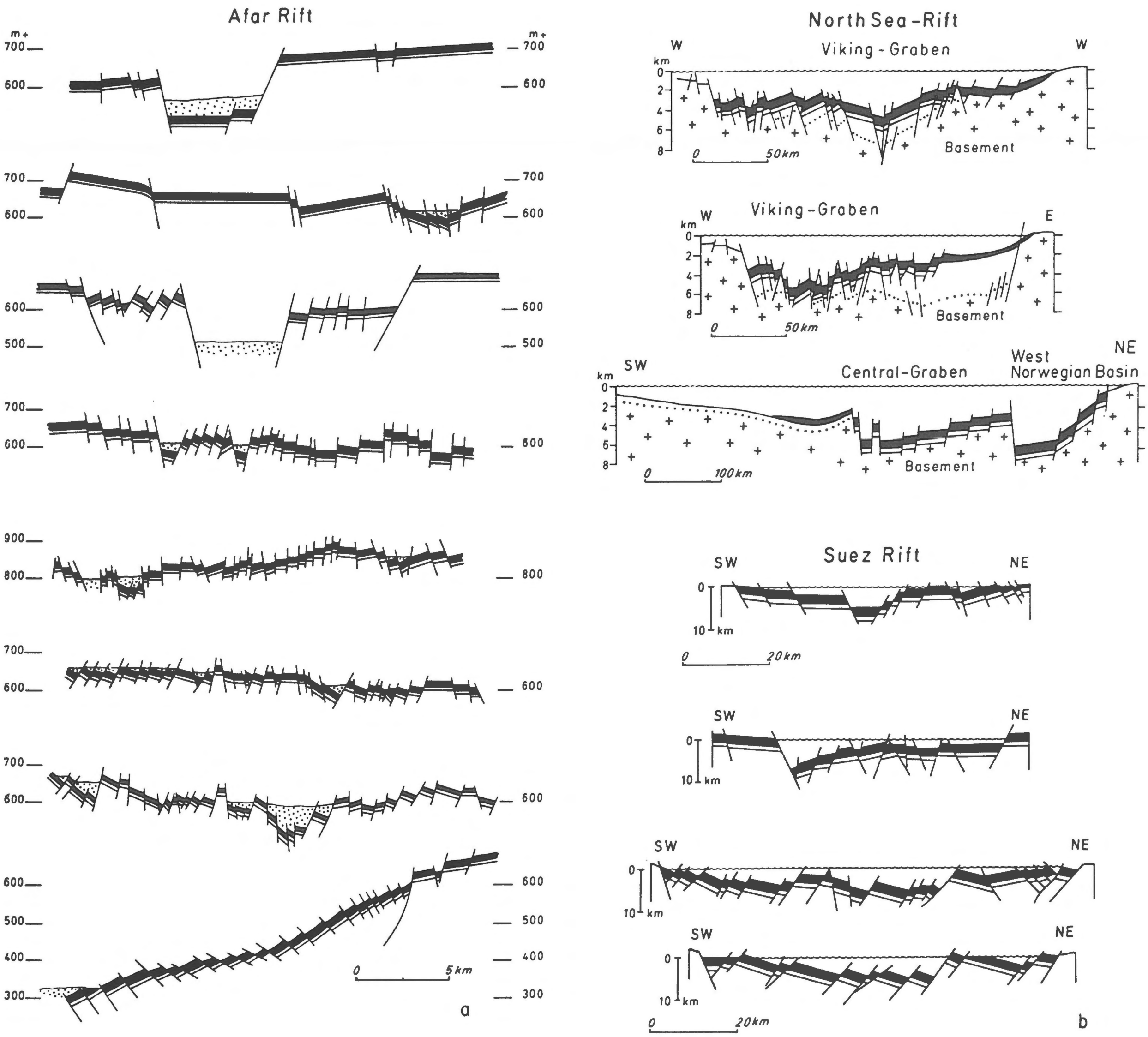

Fig. 10. For comparison: cross sections illustrating main type and stages of extensional faulting as observed and mapped on 1:50 000 aerial photography from Central Afar (Fig. 10a) and derived from borehole and geophysical data from North Sea and Suez Rifts (Fig. 10b, after Ziegler 1982, Schöneich 1988 and Coletta et al. 1988).

tings (here with visible throws of up to 1000 m) bordering major extensional units and outlining larger (internally fractured) crustal blocks, zones of uptilted imbricate fault block series, truncation of faults or fault systems, crustal flexuring (lower left corner of Fig. 8 where a high angle normal fault passes laterally into a crustal flexure) and crustal down warping (in the upper right part where sinuous fault patterns disappear under Pleistocene sediments, along strike). In Fig. 9 a LFC stereomodel demonstrates the advantage of stereoscopie view (by lens stereoscope) of structural setting and rift topography for the area between Tendaho Graben and Assal-Ghoubet Rift (compare Fig. 1b and Fig. 11). It displays, model-like, large scale crustal fragmentation, crustal warping, associated rift basins and volcanic centres. It should be pointed out that the large scale structures shown were formed under continous extension of an already intensely fractured crust and have been superimposed on

Fig. 11. LFC mosaic providing a synoptical view of Central Afar and illustrating spatial occurrence and dimensions of major extensional units, sedimentary basins and volcanic centres (compare Fig. 12). Note several photolineaments crossing regional structural units (diagonally, from upper right to lower left), indicating zones of transverse tectonic structures and associated volcanism.

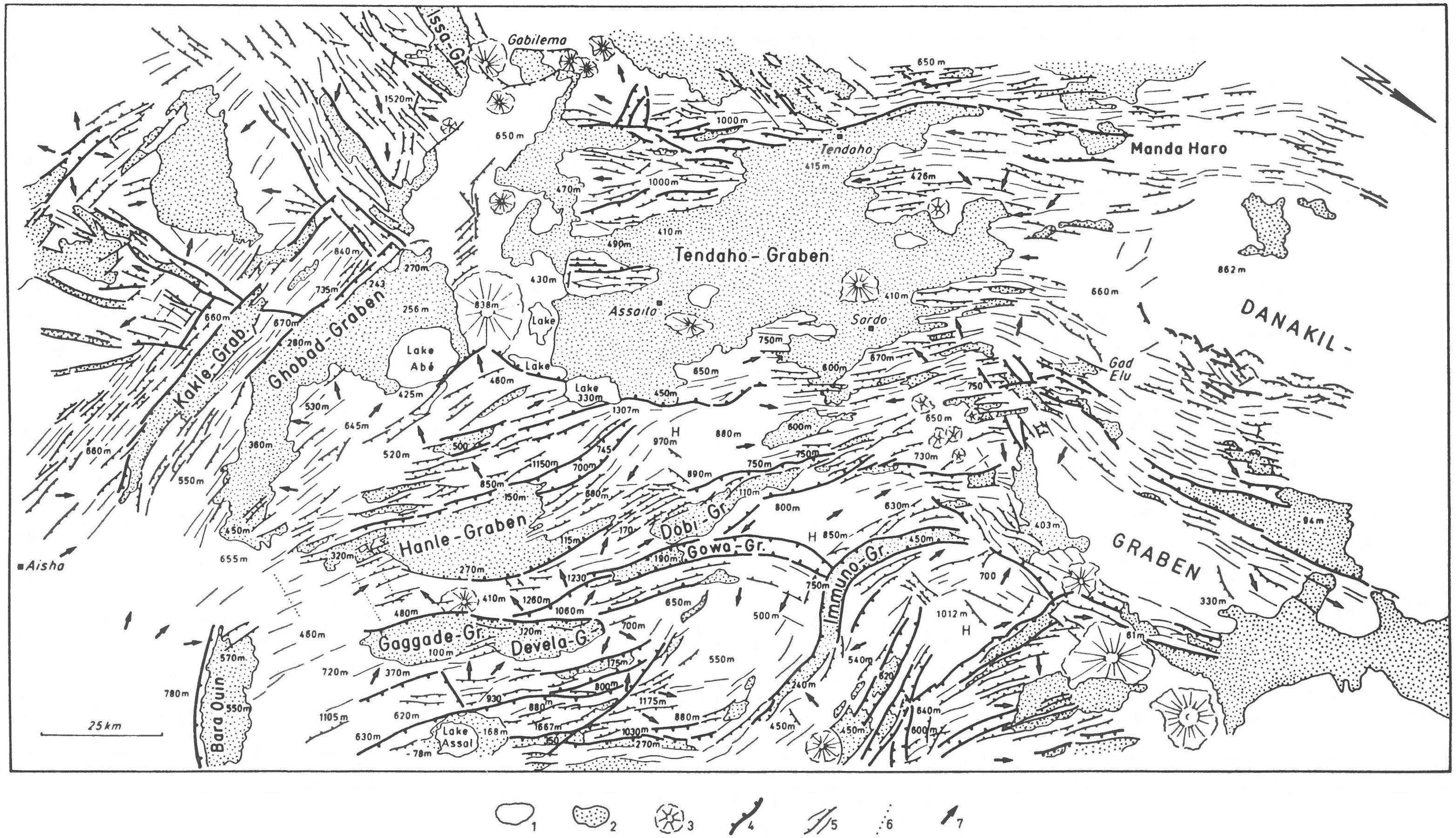

Fig. 12. Geological map of Central Afar as derived from photogeological interpretation of LFC photography (Fig. 11) displaying structural setting, sedimentary basins and major volcanic centres.

1 (white) Pliocene to Holocene volcanics, mainly stratiform basaltic rocks 2 Plio-Pleistocene sediments, fluviatile and limnic 3 Volcanic centre, mostly rhyolitic or trachytic, locally basaltic 4 regional high angle normal faults 5 extensional fault system, regional and local 6 basaltic fissures 7 dip direction of upper crust.

extensional fault geometries related to earlier phases of rifting. In this process, pre-existing faults and fault systems could have been reactivated, repeatedly, and rotated at local and regional scales. This interpretation of photogeological data is confirmed by field observations of Barberi et al. 1975, Morton & Black 1975, Christiansen et al. 1975, Black et al. 1975) from various parts of Central Afar.

In a sequence of representative cross sections Fig. 10a illustrates the principal styles and stages of upper crustal deformation observed and mapped on aerial photography (1:50 000) from Central Afar. Individual cross sections were derived from altitude measurements in stereo-models applying a stereomicrometer. Due to insufficient topographic map coverage (providing a reference base level) given altitudes have an accuracy of ± 10%. In general, Fig. 10a exhibits a wide spectrum of extensional structures and reflects inhomogeneous extension within the Central Afar rift system. From top to bottom Fig. 10a shows principle steps of progressive extensional faulting. One can observe movements of (internally faulted) larger crustal blocks across a system of a few main faults, diffuse extensional faulting with step faults, non-rotational synthetic and antithetic normal faults and associated horst/graben structures at a different scale, rotational normal faults with uniform or differential rotation of imbricate fault block sequences, roll-over geometry and half-graben configurations related to suspected listric faults, paired and multiple half-grabens and, finally, progressive rotation of imbricate fault blocks across a (suspected) listric fault. So far, little is known about Afar's extensional structures and geodynamic processes at depth, but one should expect fault plane dips of major near-surface high angle faults to decrease with depth to accomodate crustal stretching (according to well data and geophysical data from other modern rifts and extensional fault models from Wernicke & Burchfiel 1982 and Gibbs 1984). Main types of extensional fault structures shown in Fig. 10a are found in published geological cross sections from other rifts such as the North Sea- and Suez Rifts (Ziegler 1982, Schöneich 1988 and Coletta et al. 1988) at larger scales, with larger size and thickness of fault bounded crustal blocks (data in Fig. 10b derived from borehole and geophysical data). Accordingly, fault geometries shown in Fig. 10a are thought to reflect fundamental extensional mechanisms that operate at different scales and different depths in rift development.

A synoptical view at a well exposed triple junction

The LFC mosaic of Fig. 11 and a photogeological map (Fig. 12) display a synoptical aerial view of Central Afar, its structural setting, rift basins and major volcanic centres. Different trends, styles and stages of extensional faulting and superposition of fault systems are related to or are caused by differential spreading and propagation of Red Sea-, Ethiopian- and Aden Rifts, in space and time. Shown major fault systems, sedimentary basins and rift topography have resulted from upper crustal deformation during the Pleistocene and Holocene (Taieb et al. 1979, Varet 1978, Courtillot et al. 1984) whereas older rift structures, sedimentary deposits and volcanic products are covered by stratoid basalts of varying thickness ranging in age from 4.0 M.a. to 1 M.a. (Barberi et al. 1975). According to Courtillot (1982) and Makris & Ginzburg (1987) the crust of Central Afar is a stretched continental crust, about 20 km thick and underlain by a low velocity (7.4–7.5 km/s), high temperature, upper mantle. Spreading rates within Central Afar are still under discussion due to different amounts of extension in the various parts of Central Afar (Schaefer 1975) but are believed to be lower than in adjacent rift zones (Ethiopian Rift 3 mm/a, Red Sea- and Gulf of Aden Rifts about 18 mm/a as cited by Acton et al. (in press). Differential spreading of Red Sea-, Aden- and Ethiopian rift systems have caused transverse tectonical structures in the Afar rift system and in the adjacent Danakil Horst according to Barberi et al. (1975), Christiansen et al. (1975) and Tapponier & Varet (1979). The authors report on tensional and rotational movements of larger and smaller crustal blocks and associated basaltic volcanism along transversal W-E and NE-SW oriented zones.

In Fig. 11 a few major photolineaments (running

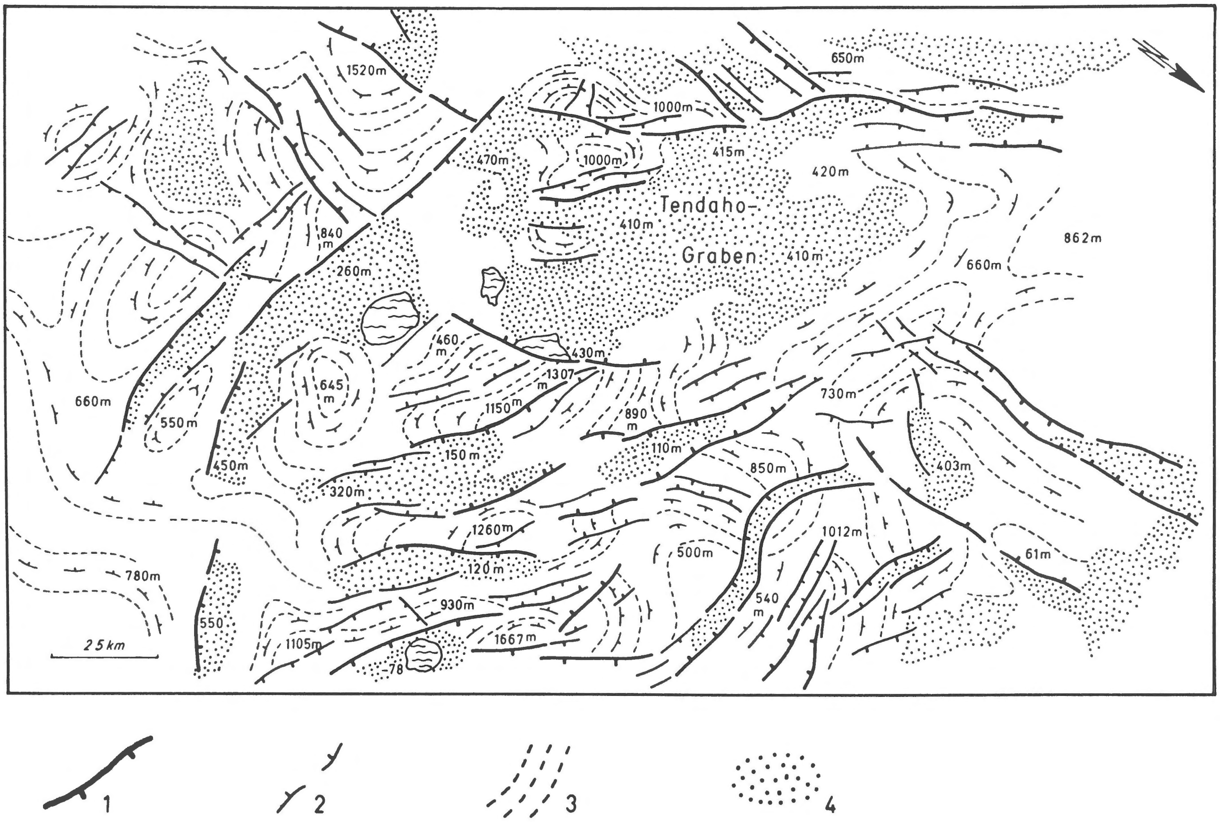

Fig. 13. Generalized structural contour map of Central Afar derived from evaluation of LFC stereo-models and elevation data from topographical maps where available (I.G.N. maps 1:100 000, 1955 and 1:200 000, 1947; Aeronautical Chart 1:1 000 000). The contour map illustrates upper crustal behaviour in an advanced rift system and triple junction characterized by intense crustal fragmentation, crustal warping and flexuring.
1 regional high angle normal faults 2 strike and dip direction of upper crustal surface 3 trends of isohypses 4 sedimentary basins

from upper right to lower left in about equidistant sets) can be traced across the LFC mosaic. These photolineaments trace W-E and WNW-ESE striking transverse zones. The most evident photolineament in the extreme right part of Fig. 11 (striking perpendicular to the regional trend of the Danakil Graben) marks the westward projection of the important W-E striking Assab-structure described by Barberi et al. (1975) with axial offsets, subrecent alkali-basalt volcanism and upward intrusion of mantle material (as shown by geophysical data and by the presence of mantle-derived peridotite inclusions in basalts from the transversal structure). Another prominent photolineament crossing, diagonally, the upper left part of Fig. 12 follows the structural trend of Kakle- and Ghobad Graben (WNW-ESE). It marks the deep- reaching crustal break outlining the border zone between Central Afar and Southern Afar (see Figs. 1b and 11). It is characterized by intense subrecent basaltic volcanism and abrupt termination of the NNW-SSE striking Tendaho Graben. In the central part of Fig. 11 WNW-ESE oriented LFC photolineaments correspond to dextral transverse faults displacing NE-SW striking Pliocene-Holocene transverse faults and dikes described by Christiansen et al. (1975).

A very generalized structural contour map (Fig. 13) derived from three-dimensional evaluation of LFC stereo-models by simple photogrammetric procedures (applying a stereomicrometer under a mirror stereoscope) displays some interesting information on upper crustal topography within the triple junction, at the regional scale. Widespread crustal subsidence with local crustal upwarping (W of Assaito see Fig. 12) characterizes the area of the Tendaho Graben. Within the adjacent part of Southern Afar (situated in the upper left part of Fig. 13) one can observe several well defined local domes surrounding a sedimentary basin reflecting an area of subsidence (sag basin?). The axial length of individual crustal highs and lows amounts to 20 or 30 km. Note the well developed graben structures across the axis of some crustal domes. In the region between the Tendaho Graben and the Southern Danakil Graben (compare Fig. 12) one can observe an E-W striking zone of moderate crustal upwarp (about 75 km in length an 25 km wide). The upper crustal high coincides with a change in directional trends of rift structures from N-S to NW-SE. It is oriented parallel to E-striking photolineaments outlining zones of transversal tectonics. Another zone of (stronger) crustal upwarp trending NNW-SSE can be traced parallel to the eastern margins of Danakil- and Tendaho Graben over a length of about 100 km at a width of about 25 km (between P. 1012 and P. 1307 in Fig. 13). Widespread crustal doming modified in its topography by abrupt subsidence of larger crustal blocks along the various major graben structures characterizes the areas around the Assal-Ghoubet Rift (lower central part of Fig. 13). One might speculate whether in an area of attenuated crust such as Central Afar (crustal thickness about 20 km) the above mentioned zones of crustal upwarp and doming might express regional and local upwelling of astenospheric material.

Acknowledgment

The work was supported by the German Research Foundation (DFG) grant Kr. 273/40-1.

References

Acton, G.D., I.F. Engeln & S. Stein (in press) Block rotation and continental extension: a microplate model for Afar – Tectonophysics (Spec. Issue on Rifting)

Barberi, F., G. Ferrara, R. Santacroce & J. Varet 1975 Structural evolution of the Afar junction. In: Pilger, A. & A. Rösler (eds): Afar Depression of Ethiopia, 1 – Inter. Un. Comm. Geodyn., Schweizerbart, Stuttgart: 38–54

Barberi, F. & J. Varet 1975 Recent volcanic units of Afar and their structural significance. In: Pilger A. & A. Rösler (eds): Afar depression of Ethiopia. 1 – Inter. Un. Comm. Geodyn., Schweizerbart, Stuttgart: 174–178

Black, R., W.H. Morton & D.C. Rex 1975 Block tilting and volcanism within the Afar in the light of recent K/Ar age data. In: Pilger, A. & A. Rösler (eds): Afar Depression of Ethiopia, 1 – Inter. Un. Comm. Geodyn., Schweizerbart, Stuttgart: 296–300

Bosworth, W. 1985 Geometry of propagating continental rifts – Nature. 310: 625–627

Bosworth, W., J.J. Lambiase & R. Keisler 1986 A new look at Gregory's Rift: The structural style of continental rifting – Eos. Trans. Am. Geophys. Un., 67, 29: 577–583

Christiansen, T.B., H.K. Schaefer & M. Schönfeld 1975 Geology of southern and central Afar, Ethiopia. In: Pilger, A. & A. Rösler (eds): Afar depression of Ethiopia, 1 – Int. Un. Comm. Geodyn., Schweizerbart, Stuttgart: 259–277

Cochran, J.R. & F. Martinez 1988 Evidence from the northern Red Sea on the transition from continental to oceanic rifting – Tectonophysics, 153: 25–53

Coletta, B., P. Le Quellec, J. Letouzey & J. Moretti 1988 Longitudinal evolution of the Suez rift structure (Egypt) – Tectonophysics, 153: 221–233

Courtillot, V. 1982 Propagating rifts and continental break-up – Tectonics, 1: 239–250

Courtillot, V., J. Achache, F. Landre, N. Bonhommet, R. Montigny & G. Feraud 1984 Episodic spreading and rift propagation: New paleomagnetic and geochronologic data from the Afar nascent passive margin – J. Geophys. Res., 89: 3315–3333

Ebinger, C.J. 1989 Tectonic development of the western branch of the East African rift system – Geol. Soc. Am. Bull., 101: 885–903

George, U. 1982 Geburt eines Ozeans – Geo. Gruner und Jahr (Hamburg): 360 pp

Gibbs, A.D. 1984 Structural evolution of extensional basin margins – Geol. Soc. Lond. J., 141: 609–620

Jackson, J. & D. McKenzie 1983 The geometrical evolution of normal fault system – J. Struct. Geol., 5: 471–482

Makris, J. & A. Ginzburg 1987 The Afar depression: Transition between continental rifting and sea-floor spreading – Tectonophysics, 141: 199–214

McClay, K.R. & P.G. Ellis 1987 Geometries of extensional fault patterns developed in model experiments – Geology, 15: 341–344

Morley, C.K. 1988 Variable extension in Lake Tanganyika – Tectonics, 7: 785–801

Morton, W.H. & R. Black 1975 Crustal attenuation in Afar. In: Pilger, A. & A. Rösler (eds): Afar depression of Ethiopia. 1 –

Inter. Un. Comm. Geodyn., Schweizerbart (Stuttgart): 55–65

Rosendahl, B.R. 1987 Architecture of continental rifts with special reference to East Africa – Ann. Rev. Earth Planet. Sci 141: 445–503

Schaefer, H.-U. 1975 Investigations on crustal spreading in southern and central Afar (Ethiopia) In: Pilger, A. & A. Rösler (eds): Afar Depression of Ethiopia. 1 – Inter. Un. Com. Geodyn. Schweizerbart (Stuttgart): 289–296

Schöneich, H. 1988 Erdöl und Erdgas im Norden Westeuropas – Die Geowissenschaften, 6: 365–376

Taieb, M., J.J. Tiercelin & H. Faure 1979 Continental sedimentary basins in East Africa (Afar) in regard to the structural evolution – In: Int. Sympos. Geodynamic evolution of the Afro-Arabian Rift System. Cons. Naz. d. Ric. Abstract, (Rome): 89 pp

Tapponnier, P. & J. Varet 1979 La zone de Mak'Arrassou en Afar: un equivalent emerge des 'failles transformantes oceaniques – C.R. Acad. Sci. (Paris) (D), 278(2): 209–212

Varet, J. 1978 Geology of central and southern Afar – Cent. Natl. Rech. Sci. (Paris): 124 pp

Wernicke, B. & B.C. Burchfiel 1982 Modes of extensional tectonics – J. Struct. Geol., 4: 105–115

Ziegler, P.A. 1982 Geological atlas of Western and Central Europe – Elsevier Sci. Publ. Co. (Amsterdam): 130 pp

Maps

Institute Geographique National 1947 Carte du Territoire Francais des Afars et de Issas. 1:200 000, Paris

Institute Geographique National 1955 Carte de la côte Francaise des Somalis, Territoire Francais des Afars et des Issas, Paris

Aeronautical Chart 1:1 000 000, ONC K5

Photography

Aerial photography 1963, 1964 – VM – VHC – M 114, 1370 PMW AF 58–3

Large Format Camera photography – NASA, STS Mission 41-G: Orbit 65, Frame Nrs. 1330–1332